Solar Energy 169 (2018) 457–467

Contents lists available at ScienceDirect

Solar Energy

journal homepage: www.elsevier.com/locate/solener

A > 3000 suns high concentrator photovoltaic design based on multiple Fresnel lens primaries focusing to one central solar cell

Katie Shanks[a,*], Juan P. Ferrer-Rodriguez[b], Eduardo F. Fernández[b], Florencia Almonacid[b], Pedro Pérez-Higueras[b], S. Senthilarasu[a], Tapas Mallick[a,*]

[a] Environmental and Sustainability Institute, University of Exeter Penryn Campus, Penryn TR10 9FE, UK
[b] Centre for Advanced Studies in Energy and Environment, University of Jaen, Campus las Lagunillas, Jaen 23071, Spain

ARTICLE INFO

Keywords:
Concentrator photovoltaics
Ultrahigh concentrator
Optical loss
Ray trace simulation

ABSTRACT

A high concentrator photovoltaic design is proposed of 5800x geometrical concentration ratio based on multiple primary Fresnel lenses focusing to one central solar cell. The final stage optic is of a novel design, made of a high refractive index (n = ~1.76), to accept light from four different directions but very easily manufactured. The high geometrical concentration of 5800x was chosen in anticipation of the losses accompanied due to alignment difficulties. Two scenarios are however simulated, one with state of the art optics (achromatic Fresnel lenses and 98% reflective mirrors) and one of standard, relatively cheap optics. An optical efficiency of ~75% is achieved in simulations if high quality optics are utilised, which gives an optical concentration ratio of just over 4300x. Simulating standard optical constraints with less accurate optics results in an optical efficiency of ~55% which translates to an optical concentration ratio of ~3000x. In this way the quality of the optics can be chosen depending on the trade of between cost and efficiency with room for future advanced optics to be incorporated at a later date. The optical efficiency of each component is simulated as well as experimentally measured to ensure the accuracy of the simulations. A theoretical acceptance angle of 0.4° was achieved in ray trace simulations for this design which is considered good for such a high concentration level. The need for achromatic Fresnel lenses is apparent from this study to reach optimum performance and concentration but even 55% optical efficiency results in a > 3000x concentration not yet experimentally tested. The solar cells irradiance distribution of the design is also presented along with performance and rough cost comparisons to other systems in the literature. The cost of the optics compared to more complex shaped optics is also given.

1. Introduction

1.1. Prospects and challenges

One trend in concentrator photovoltaic (CPV) technology is towards systems of higher concentration levels (Cristóbal et al., 2012; Shanks et al., 2016c; Vossier et al., 2012). This is due to their ability to increase cell conversion efficiencies and reduce cell size, also reducing the photovoltaic cost contribution to the full system (Gordon et al., 2004; Vallerotto et al., 2016). At present however, cheaper low efficiency solar technology such as flat plate silicon panels often win out over CPV technology despite the higher efficiencies and space conservation achieved by CPV. If an intended Solar Power installation is not restrained by space, then there is little to no motivation to install CPV over flat plate technology due to the consistently cheaper costs of flat plate PV over recent years (Ekins-Daukes, 2017; Morgan, 2017).

The work presented here focuses on a design which is relatively easy and low cost to manufacture. The design method does not prioritise optical efficiency but does incorporate the best and most likely performances due to manufacturing constraints. In this way, the cost and size (space taken up by the system) can be compared in a different manner. For example, a 1000x concentrator system which only works at 50% optical efficiency should perform as well as a perfect 100% efficient 500x design but such high efficiency optics would of course cost far more to manufacture. In which case, the less optically efficient design would be the best choice if there were no space limitations. To illustrate this further, the cost of the design presented here is given and compared to other, more complex shaped optics. This is however only one reason for exploring > 3000x concentration designs.

Multi-junction solar cells are pushing higher and higher efficiency records within relatively short time spans and need equally progressive concentrator optical designs to match. There has already been

* Corresponding authors.
E-mail addresses: K.Shanks2@exeter.ac.uk (K. Shanks), T.K.Mallick@exeter.ac.uk (T. Mallick).

https://doi.org/10.1016/j.solener.2018.05.016
Received 22 November 2017; Received in revised form 26 April 2018; Accepted 5 May 2018
Available online 13 May 2018

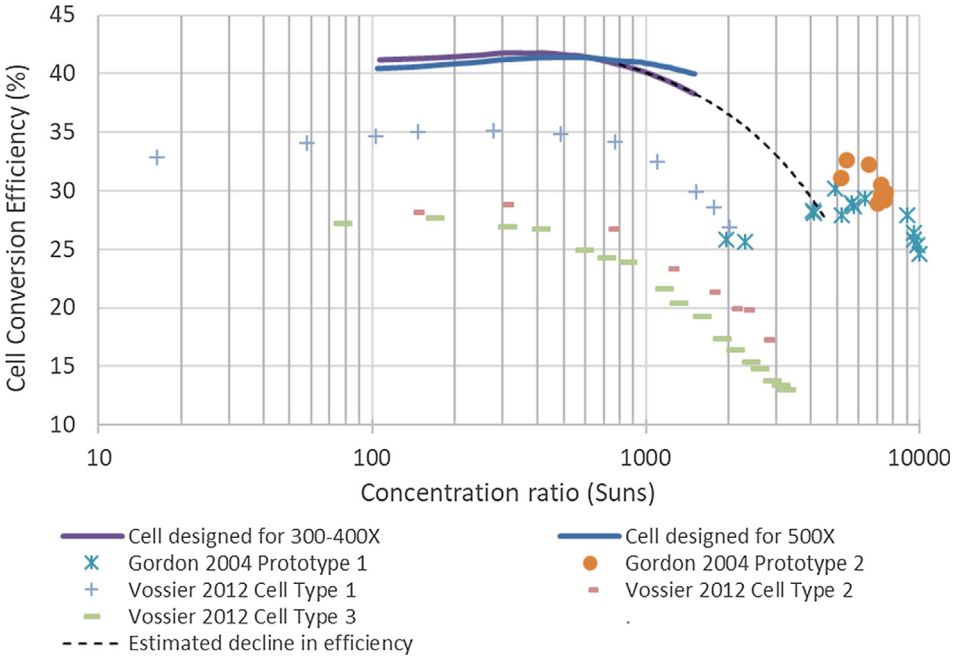

Fig. 1. Cell Conversion efficiencies at increased concentration ratios. The data for the Azur Space cells used for the preliminary experimental testing (Section 6) are given (solid lines) as well as a simple extrapolation showing the estimated decline in the efficiency (black dashed line) for the cell to be used. Experimental results from the literature are also shown for different cells and prototypes from Gordon et al. (Gordon et al., 2004) and Vossier et al. (Vossier et al., 2012) for comparison.

promising theoretical and experimental results for the efficiency of solar cells working at higher concentration ratios than which they were designed for as shown by Fig. 1. Although the results from Vossier 2012 are of lower efficiency cells, it is expected from the Azur Space cell data and Gordon 2004's results that a similar efficiency decline is possible for higher efficiency solar cells also.

At present, there lacks any reliable > 3000x CPV system to experimentally test if, in real weather conditions, very high concentration systems could produce more power and be more cost effective despite the lower conversion efficiencies of the cells. The durability of the cell and the optics for example, in varying temperatures and where light exposure will naturally rise and fall depending on cloud cover and day length, are unknown. The maximum temperature reached by concentrated light of > 3000x incident on a solar cell is one of the most important questions to be addressed and required to suitably design cooling mounts and metallization patterns for the solar cells. Literature suggests that as long as the light distribution upon the cell is distributed relatively uniform and there is sufficient cooling (passive or active), then the temperature should be manageable (Braun et al., 2013; Katz et al., 2006). There has already been research into the effect of high temperatures on Fresnel lenses (Hornung et al., 2015, 2010, 2012) and the ability of passive cooling plates to accommodate high concentration ratios up to 4000x (Micheli et al., 2016, 2015). The miniaturisation of solar concentrators in particular is a method which can significantly reduce solar cell temperatures. In which case, the proposed design here could be downscaled and enhanced further but must be proven first.

Although the system is designed for use with a multijunction solar cell, it is anticipated that thermal applications would also be of great interest under such high concentration ratios. Not only for solar-thermal power generation but for other developing thermionic metamaterials which can perform significantly more effectively at high temperatures (Andrade et al., 2014).

The main design constraint for the optics of very high (> 3000 suns) CPV systems is the difficulty to achieve a high tolerance design which is simultaneously of a high optical efficiency. This is ultimately due to the limits of etendue but are also affected by material availability and manufacturing accuracy (Languy and Habraken, 2013; Shanks et al., 2015; Vallerotto et al., 2016; Winston and Gordon, 2005).

Fresnel lenses as a primary concentrating optic have a relatively good acceptance angle and optical efficiency in comparison to the cassegrain design utilising conic primary reflectors (Shanks et al., 2016c). If used alone, a single medium Fresnel lens is limited in concentration ratio by chromatic aberration to ~1000 suns ((Languy et al., 2013). Achromatic Fresnel lenses made of 2 mediums as described by Languy et al. (Languy et al., 2013) and Guido et al. (Vallerotto et al., 2016) can achieve higher concentration ratios but are still to reach full scale manufacturing. The other option for very high concentrations is to incorporate multiple concentrating optics in a singular system but too many can significantly reduce the optical efficiency and tolerance (due to manufacturing and alignment error). In this paper we present a high concentration design of geometric concentration ratio ~5800x in anticipation of high optical losses and to compare the effects of different quality optics. In this way this study will not only present a new type of > 3000x high concentrator that can be built with current standard optics but also with developing state of the art optics to reach optimal performance. In theory, by deprioritising the optical efficiency it should also be easier to achieve a good acceptance angle for the system.

Another constraint in achieving > 3000x high concentration ratios is fabrication limits, the size of Fresnel lens or conic mirror required would be costly and difficult to manage. To overcome this, we use 4 Fresnel lenses' focusing to 1 central PV cell with the aid of other redirecting and concentrating optics (Fig. 2). A similar method has been adopted by Ferrer-Rodriguez et al. who recently proposed a design consisting of 4 cassegrain style reflectors which were angled to focus onto a central receiver optic and PV cell (Ferrer-Rodriguez et al., 2016). There has also been a design with a similar 4 entrance curved tertiary optic by Zamora et al. (Zamora et al., 2012) but this utilises a dome shaped Fresnel lens which is difficult to manufacture. The curves of the tertiary central optic would also mean a specific mould would need to be developed which has high initial costs. The design presented in this paper maintains a tertiary optic whose conic shape is simply spherical (Figs. 2, 3C and 8A) and which can be made by a common circular drill tip of the appropriate diameter. The uniqueness of this design and the optimisation method is in which the manufacturability of each component is somewhat prioritised more than the optical efficiency of those components.

Minano et al. suggest other designs following the 4 part beam splitting method which can achieve higher CAP values but all of these designs are costly to manufacture either in the primary or in the tertiary optics geometry (Minano et al., 2013). The maximum concentration

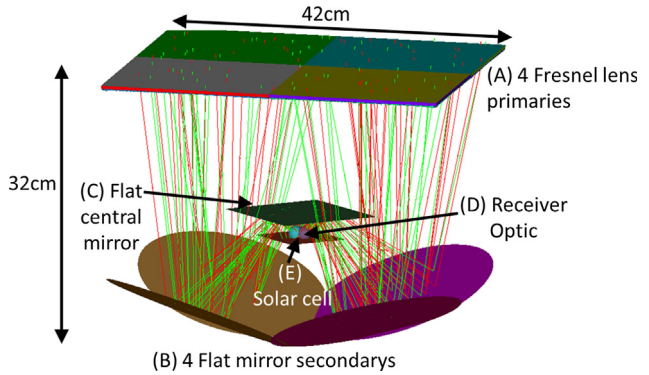

Fig. 2. Ray trace diagram of ultrahigh concentrator showing 4 square Fresnel lenses focusing towards 4 angled flat reflectors. The light it reflected again by a central flat mirror onto a central refractive optic made of 4 spherical filled lenses completing concentration onto the solar cell receiver. The green and red rays represent 400 nm and 1600 nm light respectively.

ratio theoretically achieved by the latter design is 2300x. Here we aim to achieve a higher optical concentration ratio and an acceptance angle achievable by current tracking systems ($> 0.3^{\circ}$). Mainly we have tried to maintain a relatively simple design (flat mirrors utilised for re-direction as well as the easily moulded tertiary) with standard components that can be manufactured without high initial costs for the prototyping stage. We utilised both ray trace simulations and practical testing of each component to ensure component level losses are not underestimated.

2. Design and method

For this design we chose 4 square Fresnel lenses, Silicon on glass (SOG) and also the achromatic doublet on glass (ADG) being developed by Vallerotto et al. (Vallerotto et al., 2016) with focal lengths of ~46 cm and aperture areas of 21 cm by 21 cm each. We simulated and measured silicon on glass (SOG) Fresnel lenses for the standard version of the prototype and we simulated the expected difference when using state of the art achromatic lenses. For the receiver we assume a size such as the Azur Space 5.5 × 5.5 mm multi-junction solar cell. This gives us a geometric concentration ratio of 5831x and an optical concentration of 4103 if 70% optical efficiency is obtained. To gather the light towards the centre we use flat mirrors and a central refractive optic made of 4 filled dome lenses as shown in Figs. 2c and 8a (moulded optic).

To keep the design as simple as possible and minimise loss due to manufacturing inaccuracies flat mirrors were used instead of conically shaped ones. The surface roughness for curved optics is typically higher than for flat mirrors due to manufacturing tolerances and results in a reduced reflectance when applying coatings (Shanks et al., 2016b). Polishing and smoothing these optics risks altering the specific curve which would introduce other optical inaccuracies in the system. So overall the spectral reflectance of curved mirrors is typically lower than flat mirrors or expensive to enhance. Flat mirrors are easier to manufacture and obtain in small quantities for the prototyping stage and if needed it is easier to apply high reflective film (~97%) and achieve a ~97% efficient mirror at relatively low costs. Accurately manufacturing large smooth shapes of metal is also very challenging if intending on using vacuum metalizing methods to coat the metal into a mirror (Shanks et al., 2016bb). Aligning the mirrors with their specific angle of inclination will also be easier if they are flat. In the built system however, there will always be some alignment errors, placement challenges even for pick-and-place methods as well as possible shading depending on the structural components required to hold the primary Fresnel lenses for example. A central flat mirror as the third optical stage was also chosen but mainly due to the unique quarter boundaries experienced by this design as the light rays travel close to the centre (Fig. 3A). As shown in Fig. 3A, any optic located close to the centre of the design (centre of the 4 Fresnel lenses when viewed from above) must only fill 90° of the plane or be a continuous revolution. For

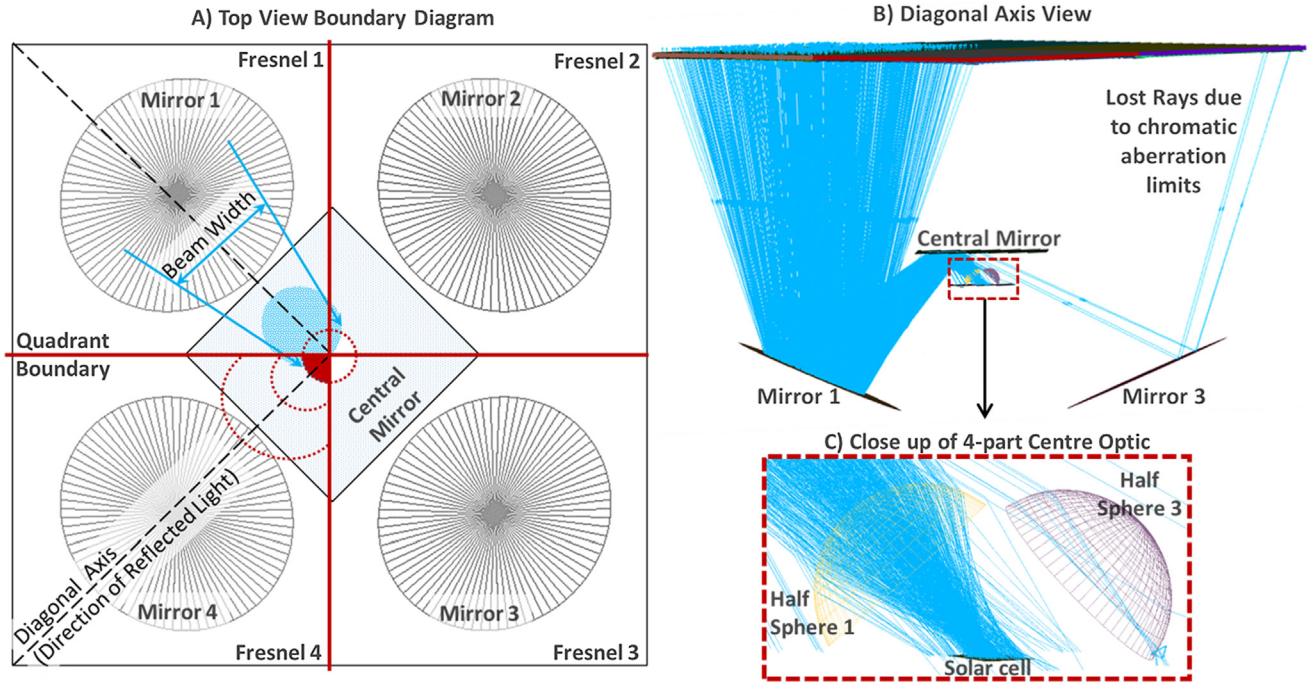

Fig. 3. (A) Top view diagram of the optical systems 4 quadrants and how light focuses onto the central mirror. The dotted red curves show examples of how an increase in the size of an offset optic will still be constrained by the quadrant boundaries. (B) Ray trace diagram viewing the diagonal face of the system where light can be seen focusing from the Fresnel lens onto the first flat mirror then the central flat mirror until finally hitting the refractive lenses. The effect of chromatic aberration is also shown. (C) Close up of the 4-part centre lenses showing only the shells of lenses 1 and 3 for simplicity. The manufactured optic is completely filled and joined to the solar cell with an optically coupling adhesive (see Fig. 8 in Section 6: Preliminary Experimental Testing).

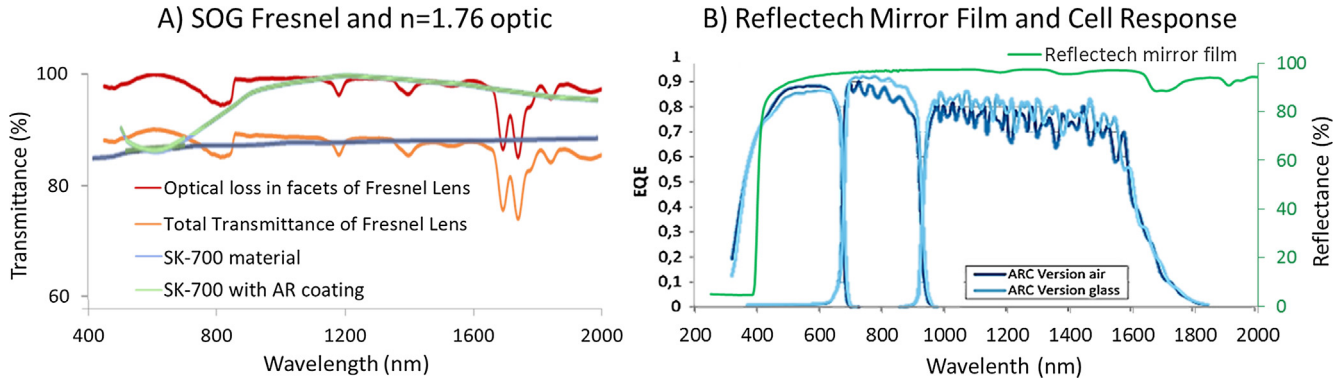

Fig. 4. (A) Measured transmittance of Fresnel lens using pane of glass as a reference to measure scattering within facets. Transmittance of material SK-700 material with refractive index 1.74–1.76 and the theoretical transmittance of such a material with antireflection coating (Leem and Yu, 2012). (B) External quantum efficiency of multi-junction solar cell from Azur Space (Azur Space Solar Power GMBH, 2014) and measured reflectance of Reflectech mirror film.

example, a half ball lens fully cantered in the middle of the Fresnel lenses would be acceptable but this does not focus the angled incoming light to the centralised solar cell.

Offset lenses can focus the incoming light to a centralised solar cell but they must fit within their quadrant. This is one of the challenges of this design linked to the width of the incoming light beam (Fig. 3A). Due to the concentration level, the limits of chromatic aberration from the Fresnel lenses and the use of only flat mirrors up until this point, the beam width overlaps into the other quadrants, especially when there is misalignment with the sun or in the optics assembly. Using the flat central mirror overcomes the boundary concern and it was ensured that its size and position did not block any rays coming from the Fresnel lens as shown in Fig. 3B at normal incidence.

The final stage optic is made of 4 truncated half sphere lenses aligned to face the incoming light as shown in Fig. 3C. Ideally this final optic will be made of a high refractive material of around 1.76 refractive index to reach maximum concentration and optical efficiency. It was also preferred to keep this refractive final stage optic small to minimise absorption losses. Larger lenses of a smaller refractive index may have worked but would also be positioned further from the solar cell and result in substantial absorption loses along with added weight and cost to the built system. Having the solar cell optically bonded (immersed) in a higher refractive index also allows for a higher concentration-acceptance product (CAP) due to the theory of etendue. Half spheres were chosen for this design due to their relatively good acceptance angle (Victoria et al., 2009) and simple shape which will be beneficial during manufacturing.

3. Ray trace simulation of system

Breault's ASAP Monte Carlo ray-tracing software was utilised along with material and component measurements to ensure the accuracy of simulation results. The light source was simulated with a spectral output of AM1.5 but shortened to optimise the priority range of 350–1800 nm for the intended solar cell and similar ranged multi-junction solar cells. The light emitted from this source was allowed a divergence angle of ± 0.27° to imitate the sun and a ray count of at least 10^6 to ensure accuracy (Cooper et al., 2013). Higher ray counts of 10^7 were used for the irradiance distributions but higher ray counts required very long processing time and computer memory. A few simulations at 10^6 and 10^8 were however compared in the early stages of simulating and showed < 0.02% change in the optical efficiency results.

Each optical interface was simulated first with the appropriate refractive index dispersions representing each of the mediums on either side of the interface. The refractive index dispersions used were mostly those included in ASAP's material library but some were inserted from previous material investigations and optical company data. The refractive index dispersion profiles allow simulations of chromatic aberration and similar optical properties as mentioned earlier. The bulk of these optics was included afterwards to ensure appropriate absorption took place. However, to simplify the simulation and reduce processing time the light path length through each optic was averaged and the absorption for each wavelength simulated using this path length instead of the software simulating unique volumetric absorptions for each ray. The full simulated transmittance was compared to the practical measurements and adjusted where needed to ensure suitable representation. Although this method should not affect the result by much when the full system is aligned at normal incident sunlight, increased incidence angles would mean different path lengths for different wavelengths through the lenses. This is something to be improved in the simulations but is not normally a significant contribution to optical losses and hence not simulated due to processing requirements. The solar cell itself was simulated as a fully absorbing material which will not be the case in practice but requires investigations beyond the scope of this paper. The type of solar cell, its materials and surface structure as well as any AR coatings and optical coupling layers joining the solar cell to the final optic need to be optimised separately and in experimental tests to gain meaningful results. The temperature management of the cell and the coupling layers joining the final optic will be important to ensure efficient thermal management and energy output from this system.

The achromatic lenses in the state of the art version of this system were simulated using the materials (PC and EVA on Glass) as designed by Vallerotto et al. (Vallerotto et al., 2016). Although they have not manufactured these lenses to the same size suggested in this paper, a few variations with appropriate refractive index dispersion curves for the materials were simulated and the one with the focal area and transmittance close enough to the performance described in their paper was used.

4. Quality and efficiency of optical components

Due to the accuracy required for these high concentrator optics, thorough simulations as well as some measured optical properties (Fig. 4) were carried out to ensure the design was modelled accurately. The quality of the optics plays a significant role in the achieved optical efficiency (Roman et al., 1995; Shanks et al., 2016a, 2016b6; Yin and Huang, 2008) and so two scenarios are given for this system – standard quality and state of the art quality optics (Fig. 5). The standard scenario assumes a standard Silicon on glass Fresnel lens as measured in Fig. 4A (~88% transmittance), ~95% reflective mirror film as measured in Fig. 4B and a refractive centre optic made of a high refractive index material (n = ~1.76) of estimated optical efficiency ~85% (Pishchik et al., 2009) also shown in Fig. 4A. These values are averages of the below spectra to state and compare easier. However, these

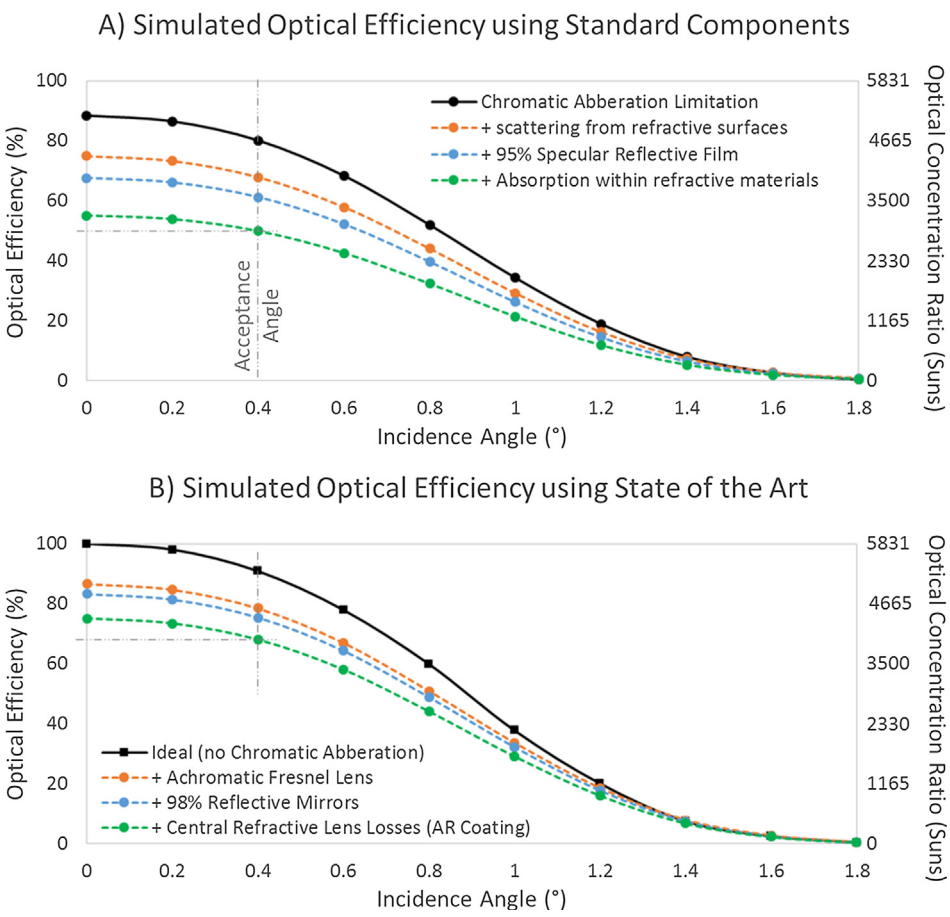

Fig. 5. (A) Simulated optical efficiency of the concentrator using standard components including a silicon on glass Fresnel lens, flat 95% reflective mirrors and an uncoated n = 1.76 centre optic. (B) The simulated optical efficiency of the system if top of the range components are utilised including an achromatic Fresnel lens made of two refractive index materials on glass, 98% silver mirrors and a high-quality n = 1.76 centre optic with an antireflective coating.

transmittance and reflectance spectra are only one part of the optical efficiency. Deviations in the light paths due to chromatic and spherical aberrations as well as coma need to be accounted for through ray trace simulation or experimental testing. In the simulations used here, each material simulated includes a reflectance spectrum so as the appropriate weighting of each wavelength progresses through the system. The wavelength range of 350–1800 nm was used in optical efficiency calculations due to this being the intended solar cell acceptance range.

The transmittance of a standard Fresnel lens is typically ~88% (Fig. 4A) and for an achromatic Fresnel lens ~86% if manufactured as suggested by Guido et al. (Vallerotto et al., 2016). Although an achromatic lens has a slightly lower transmittance, for this proposed design it would regain the scattered light due to chromatic aberration shown in Fig. 3B and C. A reflectance of > 95% should be easily achievable with flat mirrors in place. The reflectance of one of Reflectech's mirror films is shown to have slightly above this for most of the wavelength range absorbed by the intended solar cell (400–1600 nm as shown in Fig. 4B) although misses a small portion between 350 and 400 nm.

The transmittance of a high refractive index such as sapphire or SK-500, from Mitsui Chemicals, is often given to be ~85–90% as shown in Fig. 4A depending on the material purity, surface quality, thickness and temperature (Pishchik et al., 2009). This 15% loss is attributed to both scattering upon refraction into the material and due to absorption within the material. During ray trace modelling scattering and absorption effects were simulated as accurately as possible without measurements of the actual high refractive index optic to be used. These simulations suggest a scattering of ~8–14% depending on the angle of incidence and surface roughness and an internal absorption of ~8–10% depending on material composition. These results match relatively well with the properties of high refractive materials such as Sapphire and SK-500 reported in the literature (Bruns et al., 2016; Gödeker et al., 2014; Malitson, 1962; Pishchik et al., 2009). One of the interesting points of high refractive materials however is that their transmittance can be significantly increased due to the application of antireflective (AR) coatings (Bruns et al., 2016; Gödeker et al., 2014; Pishchik et al., 2009). The transmittance of the high refractive index with an AR coating given in Fig. 4A is a theoretical maximum composing of many AR layers. AR coatings can be tuned to work best for narrow ranges of wavelengths, many layers can be used to try to increase the transmittance over more of the desired wavelength range, but this becomes more expensive and difficult with each added layer. Depending on which antireflective coating is applied it may reduce the transmittance in other parts of the spectra still absorbed by the solar cell (Fig. 4B). The AR coated high refractive index transmittance given in Fig. 4A is similar to the theoretical values given in literature as well as AR modelling software completed by Brinell Vision but as stated, is a theoretical maximum given only to show the possible range of AR coatings depending on the application and budget. For the state of the art scenario simulated and presented in Fig. 5B, the scattering was assumed to be ~8% and the absorption also ~8% to give the maximum efficiency potential with a high refractive index material.

The surface quality of the high refractive index optic, wither sapphire or another material, is an unknown attribute. This as well as the optimum AR coatings to be applied to the manufactured high refractive index tertiary optic is something to be investigated in the future along with the optically coupling adhesives joining the cell to the tertiary optic. The final optical efficiency in Fig. 5A could reduce by another 4–7% if the surface roughness is higher than expected for example (Duparré et al., 2002; Pishchik et al., 2009).

In Fig. 5B the use of achromatic Fresnel lenses, 98% reflective silver mirrors and a high quality high refractive index centre optic with AR

coating increases the optical efficiency to 75.03% from the standard version of 55.12%. These values relate to an optical concentration of 4373x and 3214x respectively. The state of the art scenario is the best possible case. If an antireflective coating is not used the optical efficiency should reduce by a further 4.8% (absolute) in Fig. 5B. Both scenarios are given to show that a prototype of this system should likely fall within these two scenarios.

It should also be noted that if further corners were cut during prototype manufacturing (e.g. a cheaper low refractive index centre optic used) although this would significantly reduce the optical efficiency to ~35% this would still result in an optical concentration ratio of 2000x and could be compared in performance to similar systems and their consistency. A lower refractive tertiary optic would mean the incoming light rays from the flat mirrors (Figs. 2 and 3) would not converge enough towards the cell. The resulting distribution upon the cell area would hence in theory be more uniform and have possibly an improved acceptance angle due to a widened focal area (due to the lower refractive index) which may be necessary depending on the application and location. For the preliminary experimental investigations discussed later, a tertiary optic of refractive index ~1.5 is used to accommodate the perhaps lack of accurate alignment with in house equipment and also due to simple availability of the material at time of manufacturing.

The disadvantage of the low refractive index (35% optical efficiency) version of the system would be the waste of area used, a smaller system of higher optical efficiency could obtain the same output but could still cost more due to the manufacturing accuracy required. Depending on the aim of the design - to be most cost effective, most area efficient, or most optically efficient- different quality optics can be used. This is discussed further in Section 7 but, as a summary of the design performance, Table 1 below gives the optical efficiency, optical concentration ratio, acceptance angle and calculated optical CAP of the proposed design.

The optical CAP is the CAP calculated using the equation given in Table 1 using the optical concentration ratio instead of the geometrical concentration ratio. For a perfect CPV system of the given concentration ratio, the maximum acceptance angle allowable on earth (calculated by letting the equation given in Table 1 equal the maximum 1.76) is 1.32°. According to the definition of the CAP and the limits of etendue the absolute maximum CAP value is 1.76 for this system, equal to the refractive index within which the cell is immersed (Goldstein and Gordon, 2010; Shanks et al., 2015; Winston et al., 2005). Incorporating the geometric losses of the design, given by the upper curve of the graphs in Fig. 5A, the acceptance angle (the incidence angle with which the optical efficiency is 90% of the maximum at normal) drops to 0.4 and the CAP to 0.53. Again, with the added optical losses from state of the art optics and from standard optics, the optical efficiency, optical concentration and CAP all fall accordingly due to their direct relation to each other. A built system will fall between a CAP value of 0.46 and of 0.4 according to Table 1. This is compared to other systems in the literature in Section 7. The acceptance angle appeared to stay the same in these simulations due to the drop in maximum output at normal incidence, so the incidence angle at which 90% was achieved was still roughly 0.4 as shown in Fig. 5B. The increased Fresnel reflections and scattering due to the use of standard optics is the only optical loss that would differ from state of the art optics at increased angles of incidence of light. This loss does not appear to vary enough in comparison to the other optical losses to noticeably change the acceptance angle in these simulations. The alignment of the assembly will however affect the acceptance angle in the built system.

5. Irradiance distribution

For > 3000x high concentration the irradiance distribution and temperature of the solar cell is very important. Although the thermal performance of the solar cell is beyond the scope of this paper and requires further experimental testing with a few different solar cells and cooling methods, the irradiance distribution was considered in the design process to avoid irradiance peaks where possible. Due to the 4-separate input beams in this design, the irradiance distribution can be manipulated slightly more than usual. Depending on the angle and off-axis position of the components, especially the tertiary optics domes, the irradiance distribution can change as shown in Fig. 6 below.

The most aligned, in focus configuration resulted in Fig. 6(B) for the irradiance distribution upon the cell. This gave a higher optical efficiency but would most likely damage the solar cell. By adjusting the location of the domed lenses which make up the tertiary optic as shown in Fig. 6A, essentially moving the focal spots further apart from each other. The peak irradiance point in the centre was effectively spread out, producing a more diffused irradiance distribution as shown in Fig. 6(B)–(D). This however also slightly reduced the optical efficiency and acceptance angle of the system. Fig. 6(B) was chosen as the optimum configuration with only a 2% drop in optical efficiency. The authors note however that with further experimental testing it may be that another configuration proves to be better overall. For example, the advantage of having peaks in the corners of the solar cell may make the current and temperature dissipate slightly faster being closer to the edge of the cell. More research into this however is required.

The irradiance distribution as a function of incidence angle for the design is shown in Fig. 7.

As can be seen from the line profiles in Fig. 7 the irradiance distribution doesn't peak sharply but is a relatively gradual decline. The distribution in Fig. 7C might be an issue. This is when there is a misalignment of 0.8°. The maximum local concentrations are shown in the bottom right of each figure which reach 16 K suns in the normal incidence case and 6.4 K Suns in the 1.2° incidence angle case. So far local concentrations of up to 10 K Suns have been tested and cell damage has been avoided due to sufficient cooling (Katz et al., 2006), and cooling mounts designed for up to 4000X concentration have been designed but may not have considered maximum local concentrations (Micheli et al., 2015). Initial experimental testing (discussed in the next section) so far have not resulted in any appreciable cell damage but exposure times have been kept minimal. There was however one incidence where the temperatures caused the soldering to disengage the actual cell from the cell assembly unit. If the solar cell is kept uniformly cool then the irradiance distribution shouldn't cause too much damage to the 5.5 by 5.5 mm solar cell. Experimental testing is required to investigate this further especially due to the very high concentration levels and temperatures reachable.

6. Preliminary experimental testing

Due to the high temperatures expected from this design and the

Table 1
Concentration-acceptance angle product (CAP) analysis table depending on quality of optics used.

Simulated Design Scenario	Optical Efficiency	Optical Concentration Ratio (C_{Opt})	Acceptance Angle (°) (α)	Optical CAP ($\sqrt{C_{Opt}}\ \sin\alpha$)
Ideal (maximum theoretical limits)	100%	5831x	1.32(Etendue limit where CAP = n)	1.76 (n)
Geometric Design (No reflection or absorption losses)	100%	5831x	0.4	0.53
State of the art components (simulated)	75%	4373x	0.4	0.46
Standard component losses (simulated)	55%	3207x	0.4	0.40

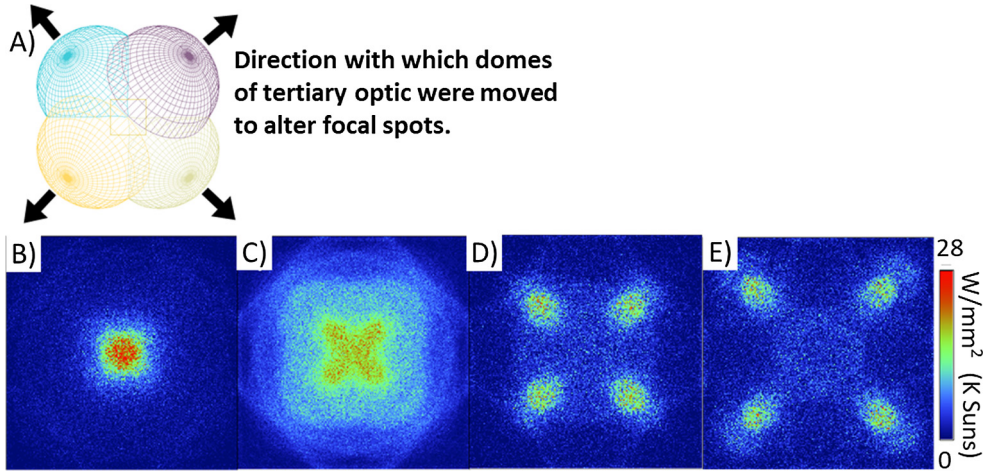

Fig. 6. Irradiance distribution upon solar cell of size 5.5 by 5.5 mm all at normal incidence alignment. (A) The direction domes of tertiary optic are moved. (B) Most focused and aligned configuration of optics. (C–E) Increasing off cantered position of half spheres which make up centre optic.

further work required on adequate cooling and solar cell design matching. Only ¼ of the system was illuminated with 1000 W/m^2 as a preliminary test of the systems concept. The first prototype was built using non-achromatic Fresnel lenses, Reflectech mirror film on metal for the flat mirrors and a moulded Sylgard 184 receiver optic. The mould for the receiver optic was manufactured in house and

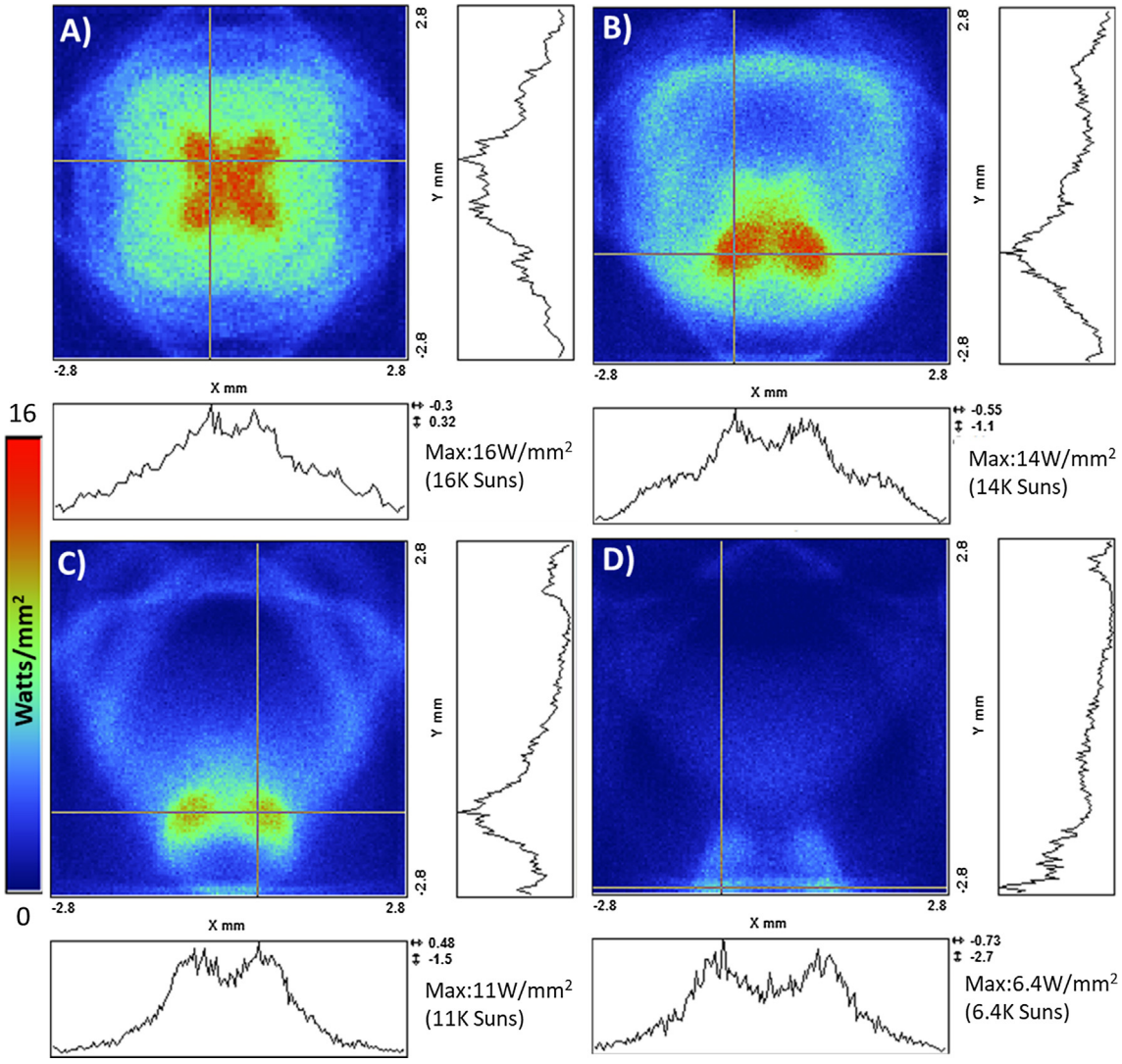

Fig. 7. Irradiance distribution on 5.5 by 5.5 mm solar cell for (A) normal incidence, (B) 0.4° incidence angle, (C) 0.8° incidence angle and (D) 1.2° incidence angle. The local maximums are shown with the crossed lines and the cross section of the intensity. These positions are also shown to the side of the distributions.

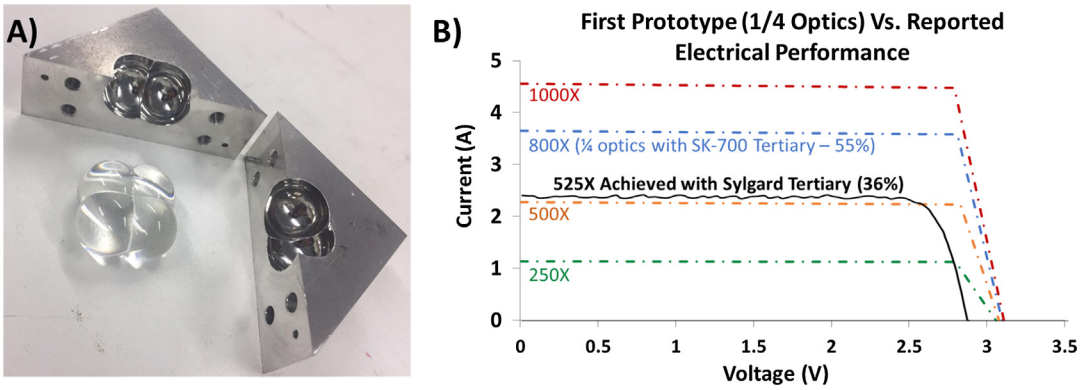

Fig. 8. (A) 4-domed tertiary optic made with two halves of drilled and polished mould. (B) I-V Trace from ¼ illumination of design compared to the reported electrical data of the solar cell from Azur Space (Azur Space Solar Power GMBH, 2014) and the estimated electrical performance with 800X optical concentration for the prototype with high refractive index tertiary.

mechanically polished (Fig. 8). Due to the simple dome curves used in the receiver optic, manufacturing was easy as was the polishing although the hand held polishing machine could still have altered the shape.

Illuminating of only ¼ of the design gives 1458X geometric concentration ratio, which drops to a ~800X optical concentration ratio when using the 55% optical efficiency given by ray trace analysis detailed previously and shown in Fig. 5A. From the data reported by Azur Space for the cell used this should give an I-V curve following close to the 800X line given in Fig. 8B. However, using Sylgard 184 with refractive index ~1.5 reduces the modelled optical efficiency down to ~35%. This fits well with the achieved I-V output given in Fig. 8B (36% back calculated optical efficiency). In fact the experimental results gave a very slightly higher output (a calculated 525X instead of the modelled 510X) which could simply be due to the uncertainty in matching the theoretical to experimental. Due to the in-house alignment capabilities, it is very likely that when aligning this prototype that the maximum output achieved is when the ¼ system is actually misaligned in favour of ¼ of the optics, and focusing the light from one Fresnel lens onto the centre of the solar cell as opposed to slightly offset which is the optimum when all 4 Fresnel lenses are in use. This of course requires further investigation and is only theoretical conjecture but seems a big coincidence that 2% optical efficiency difference is indeed gained when centring the focal point as discussed in Section 5.

The ¼ illuminated prototype produced a maximum of 2.44A (Fig. 8B) which corresponds to an estimated ~525X following its reported performance by Azur Space (Azur Space Solar Power GMBH, 2014) and the conversion efficiency of ~41.7% shown in Fig. 1. The cell should give 2.31A and 3.1 V at 500X concentration as reported by Azur Space (Azur Space Solar Power GMBH, 2014), and due to the lower voltage perhaps these loses are due to the temperature and irradiance distribution on the cell but for preliminary investigations an estimation of 525X is sufficient at this stage. Since these are preliminary tests, full detailed back calculation and determination of the solar cells exact performance efficiency was not done. This will however be under focus in the next set of investigations. From these results however, it can be extrapolated that full illumination of the prototype (all 4 lenses) would achieve at least 2100X. This concentration ratio relates to an optical efficiency of ~35% but still achieves > 2000x concentration for a relatively easily assembled design. The presumed optical efficiency of ~35% using the low refractive Sylgard material follows the predictions from the ray trace simulations described earlier. This is very reassuring for the overall design concept and accuracy of the ray trace simulations incorporating some measured optical properties. The acceptance angle of the initial prototype has not yet been accurately measured but as already said, if the low refractive index material can achieve the predicted 35% optical efficiency then any slight misalignments in this initial assembly must be within the acceptance range of the system. Although as also already stated the low refractive index version of the system would also likely have an improved acceptance angle. The raw mouldable high refractive index material is still to be attained and utilised along with the full system assembly to do further experimental testing. The alignment accuracy in this assembly was also a little limited by the equipment within our lab but will be easily improved in the next stage of experiments to achieve high performance matching simulations.

For the anticipated > 3000x concentration ratios, the results from Gordon 2004 in Section 1.1 and Fig. 1 suggest that our estimations of cell efficiency at 3000x-4000x are not impossible nor unreasonable. Furthermore, the Azur Space cell used has a top efficiency at ~400x and falls sharper than the other Azur Space cell which performs best at 500x, so higher efficiencies are instantly possible, and future work intends on comparing various solar cells under the > 3000x concentration. The Azur Space cell is used here only initially for the preliminary experimental testing.

The fact that such a result was obtained even for a very basic first prototype supports the reliability of this relatively simple but effective design incorporating flat optics. Further investigations into different solar cells, maximum temperatures reached with long exposure and the high refractive index version of the tertiary optic are required next.

7. Design comparison and discussion

A comparison table is given below (Table 2) which compares the presented design to others. As can be seen higher concentration ratios can achieve higher concentration acceptance products (CAPs) but tend to have lower optical efficiencies. This may be due to the higher number of optical stages or due to the higher priority given to maintaining an adequate acceptance angle. The number of optical interfaces shown in Table 2 includes the entrance and exit of light through the cover glass for cassegrain designs, but does not include relatively small changes in mediums such as for AR layers or within the SOG and ADG Fresnel lenses which technically have 3 and 4 medium interfaces. Interfaces between media, specifically between large differences in refractive index, will contribute to scattering and light ray deviation but careful material choice can reduce this as well as the use of AR coatings. Although this > 3000x high Fresnel lens based concentrator contains 2 flat mirrors which might seem unnecessary, the number of optical interfaces is similar to the cassegrain ultrahigh concentrator but with the advantage that the flat optics will be far easier to manufacture and position with high accuracy in comparison to the curved mirrors of the 4-off-axis-unit cassegrain design. The manufacturing difficulty is a qualitative measurement based on the need for large smooth curved optics. These are avoided in the > 3000x high Fresnel lens system

Table 2
Systems comparison table including CAP, optical efficiency, dimensions, individual system power output and comparative cost effectivity. This table assumes the cost per watt generated would be the same for each system and the bottom two rows are calculated fractions of the best CAP system, the Fresnel-Kohler design.

Concentrator Design Type	> 3000x high Fresnel lenses Concentrator under study (Theoretical)		4-off-axis-unit Cassegrain ultra-high concentrator with a central receiver (Ferrer-Rodriguez et al., 2016) (Theoretical)	Fresnel-Kohler concentrator F-RXI (Minano et al., 2013) (Theoretical)	Mini-Cassegrain Concentrator (Dreger et al., 2014) (Experimental)
Geometric Concentration Ratio	5831X		2304X	2300X	1037X
Acceptance Angle (°)	0.4		0.61	1.02	0.75
Geometric CAP	0.53		0.51	0.85	0.42
Optical Efficiency	75% (State of the Art Optics)	55% (Standard Optics)	73%	82.5%	80%
Optical Concentration Ratio	4373X	3207X	1682X	1897X	800X
Optical CAP ($\sqrt{C_{opt}}\sin\alpha$)	0.46	0.39	0.44	0.78	0.37
Solar Cell Size	5.5 × 5.5 mm		5x5mm	5.2 × 5.2 mm	1 × 1 mm
Input Aperture (m^2)	0.17638		0.0576	0.06219	0.001037
No. of Optical Interfaces	5		5	4	5
Manufacturing Difficulty	Medium	Easy	High	Very High	Medium
Cost Effectivity Comparison (Assuming Cost is higher limiting factor than land space)					
Cell Conversion Efficiency (Estimated from Fig. 1)	28%	32%	38%	36.5%	41%
System Efficiency(Cell Eff. X Optical Eff.)	21%	17.6%	27.7%	30.1%	32.8%
Input Power (1 system)	176.4 W		57.6 W	62.19 W	1.037 W
Estimated Output Power(1 system)	**42.3 W**	**31.0 W**	**17.7 W**	**21.5 W**	**0.35 W**
Power/m^2 of System	**240 W**	**176 W**	**307 W**	**347 W**	**336 W**
Number of Systems for Equal Power Generation	1.44	1.97	1.13	1	1.03
Maximum Fractional Cost required for comparative cost equality	**0.69**	**0.51**	**0.88**	**1**	**0.97**

where only a small dome shaped central optic is present. Even this is made of straightforward circular curves. There is also room for the presented design to be miniaturized such as the mini cassegrain concentrator designed by Dreger et al. (Dreger et al., 2014) where a smaller solar cell would be used and the optics downscaled which should be accompanied by reductions in cost or increases in optical quality.

As can be seen from Table 2 above, the Fresnel-Kohler concentrator F-RXI by Minano et al. (Minano et al., 2013) boasts much higher performance predictions than the other designs presented. This design follows a similar concentration method to the one presented in this paper, by which the primary optics split the light into 4 effective concentration beams and the tertiary optic reunites them upon the cell. However, the optics presented by Minano et al. are more expensive to manufacture (Minano et al., 2013) and the domed shaped Fresnel lens in the other designs more complex. The costs of these devices are unknown but the cost of the > 3000x design is given in Table 3 below along with known costs for moulds and curved mirrors to give an indication of comparison. Furthermore, a rough comparison depending on energy input, system efficiency and fractional costs is given in Table 2 above. The bottom 2 rows of which are comparing the systems to the high performing Fresnel-Kohler concentrator with the highest CAP. In this way we can see that if cost is the main priority of an intended installation, then the systems only need to be the given fractional costs of the Fresnel-Kohler concentrator to be the same cost/Watt. For example, the Mini-cassegrain concentrator by Dreger et al., 2014, only needs to cost 97% of the Fresnel-Kohler system to be equal in terms of pay back period of an installation. This is also most likely true simply due to the size of the Mini-cassegrain concentrator.

Costs can also change drastically depending on the scalability of the design. CPV technology at present however is still at a relatively low scale of production in comparison to flat plate panels. This means that most of CPV technology is made in smaller scaled production lines and of course new prototypes especially will be built in very small quantities and never benefit from large scale production savings. Yet these small prototype installations still need to out-perform current technology if they are to be taken seriously. The prototype presented here can be

Table 3
Cost of proposed design components and costs of small injection moulded glass optics and large curved plastic mirrors for comparison. The values have all been taken from companies and past purchases made. An indication of the materials and processes that can be required are given but are by no means exhaustive.

Optical Component	Processes	Materials	Initial cost (or < 100 parts)	Cost thereafter (or > 1000 parts)
SOG Fresnel Lens (4 required for 1 system)	Injection moulding	Plane Glass Silicon	< $140 (< $560 total)	< $90 (< £400 total)
Flat Mirrors (4 large and 1 small for 1 system)	Polishing and/or Coating	Sheet Metal or Plane Glass with e.g. silver/aluminium coating or mirror film	< $70 for small < $130 for large (< $570 total)	< $30 for small < $60 for large (< $250 total)
Tertiary 4-dome Central Optic (Low Refractive Index Material)	Drilling and Polishing	Aluminium Casting Material	< $90	~$8 per optic
Injection moulded glass tertiary optics	Injection Moulding	Metal (usually) Raw glass material	> $3500	$2-$10 per optic
Large curved mirrors (cassegrain system)	Metal Spinning or CNC or Coated Glass Moulds	Metal, ABS plastic coated with Aluminium/Silver (Shanks et al., 2017) or raw Glass and coating	$400-$700(for 21 × 21cm plastic mirrors)	~$140 each(vacuum metalized plastic mirrors)

made with very cheap standard optics such that the cost of < 10 systems will be far less that the cost of < 10 of any of the other systems presented in Table 2 due to the high cost of complex moulds and similar. From Table 2 it can be seen that with state of the art optics the proposed > 3000x system would be comparitively cost effective with the Fresnel-Kohler system as long as it cost 30% less to manufacture. This seems reasonable to achieve and a poorer, cheaper version would need to be 50% of the the cost of the Fresnel-Kohler system which also seems easily achievable. Perhaps the latter seems ambitious but as already stated, this design incorporates very easy optics to manufacture and the prices of which are given in Table 3 below. The mould requirement alone for the tertiary optic is only 2.4% of the cost for the mould required for the other systems so the fractional cost requirements are almost effortlessly realized. Only on orders of thousands and more would such moulds become cost effective and hence the full system more appealing. In which case the state of the art version of the > 3000x system, which may require a more expensive moulding technique for the high refractive index material, would be comparible in cost to the Fresnel-Kolher design (which also has a flat fresnel primary). The > 3000x system however has the advantage of a higher optical concentration ratio and power output per system and if both systems cost a similar amount, the cost effectivity would again be in the > 3000x systems side.

8. Conclusion

A high concentrator photovoltaic system capable of, so far unreached concentration levels, is presented and the different cases for non-ideal optics have been analyzed. The design takes advantage of flat mirrors and easy manufacturing methods in line with current and state of the art optical capabilities. The system can achieve an optical efficiency of 75% which gives ~4300x or if poorer quality optics are utilised then an optical efficiency of 55% is obtained which translates to just over 3000x. The system has an acceptance angle of 0.4° which is very good for such levels of high concentration and of a relatively simple design. Preliminary experimental tests involved an in-house built prototype which gave promising results matching the modelled 35% optical efficiency. The initial prototype has still to be developed fully but the initial results indicate the design concept is on the right track for > 3000x concentration and performance as predicted by the simulations. The design should be easy to manufacture and will be very useful in pushing CPV technology to higher concentration ratios. A comparison to other designs was also undertaken and shows high concentration designs achieving higher concentration acceptance products but their cost on an individual system level needs to be considered during design to benefit the progress of CPV technology further.

Acknowledgements

This research is funded by EPSRC (EP/P003605/1) through the Joint UK-India Clean Energy Centre (JUICE). In the support of open access research all underlying materials (such as data, samples or models) can be accessed upon request via email to the corresponding author.

References

Andrade, H.D., Othman, M.Z., Donnell, K.M.O., Lay, J.H., May, P.W., Fox, N.A., Morin, J., Renault, O., 2014. Use of energy-filtered photoelectron emission microscopy and Kelvin probe force microscopy to visualise work function changes on diamond thin films terminated with oxygen and lithium mono-layers for thermionic energy conversion. Int. J. Nanotechnol. 796–807.

Azur Space Solar Power GMBH, 2014. Enhanced Fresnel Assembly - EFA Type: 3C42A – with 5.5x5.5mm2 CPV TJ Solar Cell Application: Concentrating Photovoltaic (CPV) Modules.

Braun, A., Hirsch, B., Vossier, A., Katz, E.A., Gordon, J.M., 2013. Temperature dynamics of multijunction concentrator solar cells up to ultra-high irradiance 202–208. doi:10.1002/pip.

Bruns, S., Vergöhl, M., Zickenrott, T., Bräuer, G., 2016. Deposition of abrasion resistant single films and antireflective coatings on sapphire. Surf. Coatings Technol. 290, 10–15. http://dx.doi.org/10.1016/j.surfcoat.2015.11.011.

Cooper, T., Dähler, F., Ambrosetti, G., Pedretti, A., Steinfeld, A., 2013. Performance of compound parabolic concentrators with polygonal apertures. Sol. Energy 95, 308–318. http://dx.doi.org/10.1016/j.solener.2013.06.023.

Cristóbal, A., Martí Vega, A., Luque López, A. (Eds.), 2012. Next Generation of Photovoltaics, Springer Series in Optical Sciences. Springer-Verlag, Berlin Heidelberg, Berlin, Heidelberg. doi:10.1007/978-3-642-23369-2.

Dreger, M., Wiesenfarth, M., Kisser, A., Schmid, T., Bett, A.W., 2014. Development And Investigation Of A CPV Module With Cassegrain Mirror Optics, in: CPV-10.

Duparré, A., Ferre-Borrull, J., Gliech, S., Notni, G., Steinert, J., Bennett, J.M., 2002. Surface characterization techniques for determining the root-mean-square roughness and power spectral densities of optical components. Appl. Opt. 41, 154–171. http://dx.doi.org/10.1364/AO.41.000154.

Ekins-Daukes, N., 2017. Cost Requirements for High Volume CPV Manucaturing, in: AIP-13th International Conference on Conentrator Photovoltaic Systems (CPV-13). Ottowa.

Ferrer-Rodriguez, J.P., Fernandez, E.F., Almonacid, F., Perez-Higueras, P., 2016. Optical design of a 4-Off-axis-unit cassegrain ultra- high CPV module with central receiver. Opt. Lett. 41, 3–6.

Gödeker, C., Schulz, U., Kaiser, N., Tünnermann, A., 2014. Antireflection coating for sapphire with consideration of mechanical properties. Surf. Coatings Technol. 241, 59–63. http://dx.doi.org/10.1016/j.surfcoat.2013.07.001.

Goldstein, A., Gordon, J.M., 2010. Double-tailored nonimaging reflector optics for maximum-performance solar concentration. J. Opt. Soc. Am. A. Opt. Image Sci. Vis. 27, 1977–1984. http://dx.doi.org/10.1364/JOSAA.27.001977.

Gordon, J.M., Katz, E. a., Feuermann, D., Huleihil, M., 2004. Toward ultrahigh-flux photovoltaic concentration. Appl. Phys. Lett. 84, 3642. doi:10.1063/1.1723690.

Hornung, T., Bachmaier, A., Nitz, P., Gombert, A., 2010. Temperature and wavelength dependent measurement and simulation of Fresnel lenses for concentrating photovoltaics, in: Wehrspohn, R.B., Gombert, A. (Eds.), International Society for Optics and Photonics, p. 77250A. doi:10.1117/12.854499.

Hornung, T., Kiefel, P., Nitz, P., 2015. The distance temperature map as method to analyze the optical properties of Fresnel lenses and their interaction with multijunction solar cells. AIP Publishing, p. 70001. doi:10.1063/1.4931538.

Hornung, T., Steiner, M., Nitz, P., 2012. Estimation of the influence of Fresnel lens temperature on energy generation of a concentrator photovoltaic system. Sol. Energy Mater. Sol. Cells 99, 333–338. http://dx.doi.org/10.1016/j.solmat.2011.12.024.

Katz, E.A., Gordon, J.M., Tassew, W., Feuermann, D., 2006. Photovoltaic characterization of concentrator solar cells by localized irradiation. J. Appl. Phys. 100, 1–8. http://dx.doi.org/10.1063/1.2266161.

Languy, F., Habraken, S., 2013. Nonimaging achromatic shaped Fresnel lenses for ultrahigh solar concentration. Opt. Lett. 38, 1730–1732. http://dx.doi.org/10.1364/OL.38.001730.

Languy, F., Lenaerts, C., Loicq, J., Thibert, T., Habraken, S., 2013. Performance of solar concentrator made of an achromatic Fresnel doublet measured with a continuous solar simulator and comparison with a singlet. Sol. Energy Mater. Sol. Cells 109, 70–76. http://dx.doi.org/10.1016/j.solmat.2012.10.008.

Leem, J.W., Yu, J.S., 2012. Superhydrophilic sapphires for high- performance optics. Opt. Exp. 20, 769–773.

Malitson, I.H., 1962. Refraction and dispersion of synthetic sapphire. J. Opt. Soc. Am. 52, 1377. http://dx.doi.org/10.1364/JOSA.52.001377.

Micheli, L., Fernández, E.F., Almonacid, F., Mallick, T.K., Smestad, G.P., 2016. Performance, limits and economic perspectives for passive cooling of High Concentrator Photovoltaics. Sol. Energy Mater. Sol. Cells 153, 164–178. http://dx.doi.org/10.1016/j.solmat.2016.04.016.

Micheli, L., Micheli, L., Fernandez, E.F., Almonacid, F., 2015. Enhancing Ultra-High CPV Passive Cooling Using Least- Material Finned Heat Sinks, in: CPV-11. Aix-les-Bains, France.

Minano, J.C., Benitez, P., Zamora, P., Buljan, M., Mohedano, R., Santamaria, A., 2013. Free-form optics for Fresnel-lens-based photovoltaic concentrators. Opt. Exp. 21, A494–A502. http://dx.doi.org/10.1364/oe.21.00a494.

Morgan, J.P., 2017. Why Hasn't CPV Taken Off Yet and Will the Future Look Different, in: AIP-13th International Conference on Conentrator Photovoltaic Systems (CPV-13). Ottowa.

Pishchik, V., Lytvynov, L.A., Dobrovinskaya, E.R., 2009. Properties of Sapphire, in: Sapphire: Material, Manufacturing, Applications. Springer, US, pp. 55–176. doi:10.1007/978-0-387-85695-7.

Roman, R.J., Peterson, J.E., Goswami, D.Y., 1995. An off-axis cassegrain optimal design for short focal length parabolic solar concentrators. J. Sol. Energy Eng. 117, 51. http://dx.doi.org/10.1115/1.2847742.

Shanks, K., Baig, H., Senthilarasu, S., Reddy, K.S., Mallick, T.K., 2016a. Conjugate refractive–reflective homogeniser in a 500× Cassegrain concentrator: design and limits. IET Renew. Power Gener. 10, 440–447. http://dx.doi.org/10.1049/iet-rpg.2015.0371.

Shanks, K., Baig, H., Singh, N.P., Senthilarasu, S., Reddy, K.S., Mallick, T.K., 2017. Prototype fabrication and experimental investigation of a conjugate refractive reflective homogeniser in a cassegrain concentrator. Sol. Energy 142, 97–108. http://dx.doi.org/10.1016/j.solener.2016.11.038.

Shanks, K., Sarmah, N., Ferrer-Rodriguez, J.P., Senthilarasu, S., Reddy, K.S., Fernández, E.F., Mallick, T., 2016b. Theoretical investigation considering manufacturing errors of a high concentrating photovoltaic of cassegrain design and its experimental validation. Sol. Energy 131, 235–245. http://dx.doi.org/10.1016/j.solener.2016.02.050.

Shanks, K., Senthilarasu, S., Mallick, T.K., 2016c. Optics for concentrating photovoltaics: trends, limits and opportunities for materials and design. Renew. Sustain. Energy

Rev. 60, 394–407. http://dx.doi.org/10.1016/j.rser.2016.01.089.
Shanks, K., Senthilarasu, S., Mallick, T.K., 2015. High-Concentration Optics for Photovoltaic Applications, in: Pérez-Higueras, P., Fernández, E.F. (Eds.), High Concentrator Photovoltaics: Fundamentals, Engineering and Power Plants, Green Energy and Technology. Springer International Publishing, Cham, pp. 85–113. doi:10.1007/978-3-319-15039-0.
Vallerotto, G., Victoria, Marta., Askins, S., Herrero, R., Dominguez, C., Anton, I., Sala, G., 2016. Design and modeling of a cost-effective achromatic Fresnel lens for concentrating photovoltaics. Opt. Exp. 24, 89–92.
Victoria, M., Domínguez, C., Antón, I., Sala, G., 2009. Comparative analysis of different secondary optical elements for aspheric primary lenses. Opt. Exp. 17, 6487–6492.
Vossier, A., Chemisana, D., Flamant, G., Dollet, A., 2012. Very high fluxes for concentrating photovoltaics: considerations from simple experiments and modeling. Renew. Energy 38, 31–39. http://dx.doi.org/10.1016/j.renene.2011.06.036.
Winston, R., Gordon, J.M., 2005. Planar concentrators near the étendue limit. Opt. Lett. 30, 2617–2619.
Winston, R., Miñano, J.C., Benítez, P., Shatz, N., Bortz, J.C., 2005. Nonimaging Opt. Elsevier, Nonimaging Optics 10.1016/B978-012759751-5/50013-0.
Yin, L., Huang, H., 2008. Brittle materials in nano-abrasive fabrication of optical mirror-surfaces. Precis. Eng. 32, 336–341. http://dx.doi.org/10.1016/j.precisioneng.2007.09.001.
Zamora, P., Benítez, P., Yang, L., Miñano, J.C., Mendes-Lopes, J., Araki, K., 2012. Photovoltaic performance of the dome-shaped Fresnel-Köhler concentrator 84680D. doi:10.1117/12.929698.